Scientia Pharmaceutica

ÖSTERREICHISCHE PHARMAZEUTISCHE GESELLSCHAFT

MDPI

Article

Pharmaceutical Development and Characteristics of Orally Disintegrating Tablets with Dihydroquercetin Formulation Modifications

Roman P. Terekhov [1,*], Maria D. Korochkina [1], Elizaveta V. Krivozubova [1], Grigory Yu. Evzikov [2], Artem A. Svotin [1], Maria N. Anurova [1] and Irina A. Selivanova [1]

[1] Nelyubin Institute of Pharmacy, Sechenov First Moscow State Medical University, Trubetskaya Str. 8/2, 119991 Moscow, Russia
[2] Department of Nervous Diseases, Sechenov First Moscow State Medical University, Trubetskaya Str. 8/2, 119991 Moscow, Russia
* Correspondence: terekhov_r_p@staff.sechenov.ru; Tel.: +7-(499)-749-79-91

Abstract

Oral diseases cause a wide range of difficulties for patients. The natural bioactive compound dihydroquercetin (DHQ), which demonstrates regenerative, anti-inflammatory, antioxidative, and antibacterial effects, is of interest for their treatment. The combination of DHQ and L-lysine DHQ is "very easily soluble". The aim of this study is to compare orally disintegrating tablets based on raw DHQ and on the DHQ-L-lysine composition. Following the guidelines outlined in the ICH Q8 (R2) standard, a fundamental quality target product profile and critical quality attributes were established. The Sediment Delivery Model (SeDeM) method was used to evaluate the substance suitability for direct compression. Quantitative analysis of the DHQ release was carried out by high-performance liquid chromatography, and infrared (IR) spectroscopy was performed using the attenuated total reflection technique without any prior sample preparation. The DHQ-L-lysine composition shows improved dimensions (4.12) and flowability (4.96). The release rate constants ($K_{release}$) were 8.14 and 3.61%/min, while the half-release periods ($t_{50\%}$) were 6.14 and 13.85 min for tablets with DHQ (TF1) and DHQ-L-lysine compositions (TF2), respectively. The difference factor (f_1) and similarity factor (f_2) were 23.43% and 43.37%, respectively. The tablet manufacture had a critical impact on the characteristics of the IR spectra (the r values −0.8785 and 0.5474 for TF1 and TF2). The conducted study demonstrates the promise of using DHQ-L-lysine composition for developing effective dosage forms with improved technological characteristics and controlled release of the active substance.

Keywords: dihydroquercetin; lysine; phase modification; orally disintegrating tablets; solubility; IR-spectroscopy; flavonoids

Academic Editor: Susi Burgalassi

Received: 19 May 2026
Revised: 7 July 2026
Accepted: 8 July 2026
Published: 9 July 2026

1. Introduction

Inflammatory oral diseases are a significant challenge for modern medical science. Oral diseases are among the most common pathological states, especially in older adults, affecting about 90% of the global population at some point in their lives, with about 14% of cases (periodontitis, gingivitis, etc.) being directly related to inflammatory oral diseases. In addition, other pathological states can also lead to inflammation in the oral cavity. Furthermore, clinical evidence of some inflammatory oral diseases can be found in almost all adults, even if they have not been diagnosed with them [1–3].

There are several factors leading to inflammatory oral diseases: common risk factors (tobacco use, poor diet, etc.), poor oral hygiene, infections [4], uncontrolled diabetes mellitus [5,6], a dysregulated hyper-inflammatory response, plaque biofilm accumulation at the gingiva–tooth interface, neglected dental caries, rare syndromes, and disorders of collagen metabolism and neutrophil function [7].

Oral diseases, and inflammatory oral diseases in particular, cause a wide range of difficulties for patients, such as a negative impact on psychological state, painful sensations [1], systemic inflammation [8], bleeding, tooth loss (up to complete edentulism), and destruction of nearby tissues [3].

Inflammatory oral diseases are commonly treated with antibiotics and antiseptics (chlorhexidine, doxycycline, metronidazole, etc.) [9,10]. Antibiotic administration disturbs the oral microflora and can lead to physiological disorders and bacterial or fungal infections [11,12]. Moreover, antibiotics are frequently associated with side effects such as gastrointestinal symptoms, abdominal pain, and diarrhea [13].

Another way to treat inflammatory oral diseases is laser therapy, which provides an anti-infective effect. However, some types of laser therapy, such as low-energy and Nd:YAG lasers and photodynamic therapy, have shown no significant results and, consequently, can be used only as adjunctive therapy. Other types (diode and CO_2 lasers), meanwhile, can cause excessive heat and root damage [9].

Other methods, such as dietary changes or improved oral hygiene, are also used in clinical practice but require a higher level of patient involvement and discipline [14].

Due to the complicated etiology and accompanying negative effects, it is reasonable to combine etiological treatment of inflammatory oral diseases with symptom-managing therapy [15]. Against the background of growing interest in phytotherapy, natural bioactive compounds such as flavonoids, which have a high safety profile, are of interest in wound healing [16,17]. Particularly promising is dihydroquercetin (DHQ), the major flavonoid component of larch wood, which demonstrates skin-regenerative [18,19], anti-inflammatory [20–22], antioxidative [23,24], and antibacterial [25,26] effects—all of which are crucial in the treatment of inflammatory oral diseases.

According to opinion of some researchers [27], poor solubility in water at room temperature [28] ("very slightly soluble" according to the European Pharmacopoeia) is one of the reasons for the low bioavailability of DHQ, which makes it challenging to develop medications based on this compound and integrate them into clinical practice. There are several approaches that were previously applied to improve the solubility of flavonoids, including solid dispersion preparation [29,30], amorphization [31,32], glycosylation [33,34], and crystallization [35,36].

The proteinogenic amino acid L-lysine may also be beneficial for reducing inflammation [37]. In combination with L-lysine (DHQ-L-lysine), DHQ becomes "very easily soluble" according to the European Pharmacopoeia due to the formation of hydrogen bonds [38,39]. Previous studies have shown that the topical application of a DHQ-L-lysine composition solution was beneficial for wound healing in rats compared to the initial substances [39].

However, the influence of the DHQ-L-lysine composition on the pharmaceutical–technological properties of orally disintegrating tablets has not yet been studied. Therefore, the aim of this study is to conduct a comparative analysis of tablets based on raw DHQ and on the DHQ-L-lysine composition.

2. Materials and Methods

2.1. Materials

DHQ was provided by JSC "Ametis" (Blagoveshchensk, Russia), L-lysine was acquired from NeoFroxx GmbH (Darmstadt, Germany), high-functionality excipient PROSOLV®

ODT G2 was purchased from JRS PHARMA GmbH & Co. KG (Rosenberg, Germany), ascorbic acid was supplied by Tereos S.A. (Moussy-le-Vieux, France), and sucrose was from the Northeast Pharmaceutical Group Co., Ltd. (Shenyang, China).

Distilled water was produced before use, acetonitrile—99.9% (HPLC Gradient Grade) was acquired from Fisher Scientific (Loughborough, UK), and trifluoroacetic acid—98% was provided by Pallav Chemicals & Solvents Pvt. Ltd. (Mumbai, India). For HPLC analysis the water was deionized by Vodoley-M (Himelectronica SPE, Moscow, Russia).

2.2. Tableting Formulations Based on DHQ Modifications

Tablets were manufactured from tableting masses 1 and 2 (Table 1) by direct compression using a laboratory-scale hydraulic press 660 (Silfradent S.R.L., Santa Sofia, Italy) at a pressure of approximately 20 kN (2 tons). The tableting masses were mixed at 40 rpm for 20 min in YB-5 Mixer (ERWEKA GmbH, Heusenstamm, Germany).

Table 1. The formulations of tableting masses.

Ingredients	Weight, mg	
	Formulation 1	Formulation 2
DHQ	50	50
L-lysine	-	54
PROSOLV® ODT G2	300	300
Ascorbic acid	150	150
Sucrose	1054	1000
Total	1554	1554

2.3. Quality by Design Application to the Formulation Development

Following the guidelines outlined in the ICH Q8 (R2) standard [40], a fundamental quality target product profile (QTPP) and critical quality attributes (CQAs) have been established. QTPP elements are presented in Table 2. CQAs included the characteristics of the tablet mass and dosage form, namely crushing strength and disintegration time.

Table 2. QTTP for DHQ orally disintegrating tablets.

QTTP Elements	Target
Dosage form	Orally disintegrating tablets
Route of administration	Oral
Dosage strength	50 mg
Shape	Tablet diameter 17 mm
Disintegration time	Not more than 3 min
Population	Any age

2.4. Powder Characterization Using SeDeM Expert System

The Sediment Delivery Model (SeDeM) method was used to evaluate the suitability of both DHQ and DHQ-L-lysine composition for direct compression. For powder evaluation, 12 different parameters were identified and classified according to five factors of occurrence based on the physical characteristics of the powder and the functional properties of the drug. The numerical value for each factor represents the average value obtained from the corresponding parameter values, known as the mean dispersion radius. Once the parameter values were obtained, they were transformed into radius values (r) for graphical

representation. The parameters presented in Table 3 were defined according to the European Pharmacopoeia and other sources [41].

Table 3. The SeDeM expert system parameters.

Parameter	Symbol	Unit	Equation	Acceptable Ranges	Conversion to *r* Equation
Bulk density	Da	g/mL	$Da = m/V0$	0–1	$10Da$
Tapped density	Dc	g/mL	$Dc = m/V1250$	0–1	$10Dc$
Interparticle porosity	Ie	-	$Ie = (Dc - Da)/(Dc \times Da)$	0–1.2	$10Ie/1.2$
Carr index	IC	%	$IC = ((Dc - Da)/Dc) \times 100$	0–50	$IC/5$
Cohesion index	Icd	N	Experimental	0–200	$Icd/20$
Hausner index	IH	-	$IH = Dc/Da$	3–1	$(30 - 10IH)/2$
Angle of repose	α	○	Experimental	50–0	$10 - (\alpha/5)$
Powder flow	t''	s	Experimental	20–0	$10 - (t''/2)$
Loss on drying	$\%HR$	%	Experimental	10–0	$10 - \%HR$
Hygroscopicity	$\%H$	%	Experimental	20–0	$10 - (\%H/2)$
Particles < 50 µm	$\%Pf$	µ	Experimental	50–0	$10 - (\%Pf/5)$
Homogeneity index	$I\theta$	-	$I\theta = Fm/(100 + \Delta Fmn)$	0–0.02	$500I\theta$

The Good compression index (*IGC*) to numerically assess the powder's appropriateness for direct compression was calculated according to the following formula:

$$IGC = IPP \times f \quad (1)$$

where *IPP* is the parametric profile index, representing the mean value of all calculated parameters, and f is the reliability factor, determined by the ratio of polygon area to circle area (*const* 0.952 for 12 parameters).

The acceptability limit of *IPP* is set at $r \geq 5$.

2.5. Flowability of Tableting Masses

To determine the flow rate of tableting masses through an orifice, a Granulate Flow Tester GTB ERWEKA GmbH (Heusenstamm, Germany) and a stainless acid-resistant steel funnel of the "hopper" type (without an outlet stem) with an orifice diameter of 10 mm were used. A paper substrate was used as the base. A 100 g sample, weighed with a precision of ±0.5%, was placed into the dry funnel. The time required for the entire sample to pass through the funnel orifice was recorded. The test was performed in triplicate for each sample.

After each flow rate measurement, the angle of repose was determined using a goniometric scale.

To determine the bulk volume of the tableting mass, a sample aliquot was weighed and poured into a 25 mL graduated cylinder. The tapped density tester SVM 102 (ERWEKA GmbH, Heusenstamm, Germany) was used to determine the volume of the tableting mass after compaction. The previously weighted tableting mass was placed into a 25 mL graduated cylinder, which was then fixated on the device and subjected to up to 1250 taps. Afterwards, the volume was measured. The experiment duration for each sample was 5 min. The test was performed in triplicate for each sample.

The bulk density (*Da*, g/mL) and the tapped density (*Dc*, g/mL) were calculated using the formulas presented in Table 3, where *m* is weight of the test sample (g), *V*0 is the bulk volume of the tableting mass (mL), and *V*1250 is the volume of the tableting mass after compaction (mL).

Carr's index (*IC*) and the Hausner index (*IH*) were calculated using the formulas in Table 3.

2.6. Pharmaceutical–Technological Characteristics of Tablets

The quality control of orally disintegrating tablets was guided by the European Pharmacopoeia [42].

2.6.1. Disintegration

To perform the disintegration experiment, a ZT 121 light tester (ERWEKA GmbH, Langen, Germany) of the oscillating basket type was used. The volume of purified water in the beaker was 900 mL, with the temperature maintained at 37 ± 2 °C. Six tablets of each formulation were subjected to the test. Each tablet was placed into a tube of the oscillating basket and analyzed for 45 min.

2.6.2. Crushing Strength

The tablet hardness tester TBH 125 (ERWEKA GmbH, Langen, Germany) was used to measure the exact diameter of the tablets and their crushing strength. The test was conducted on ten tablets of each formulation. Since the tablets had a score line (indentation), each one was oriented identically with respect to the direction of the applied force.

2.6.3. Friability

The friability test was performed on ten tablets of each formulation using a friability and abrasion tester TAR 220 (ERWEKA GmbH, Langen, Germany). The tablets were first weighed to an accuracy of 0.001 g and then dusted off. The drum rotation speed was set to 25 revolutions per minute (rpm). The experiment duration was 4 min. After the specified time had elapsed, the tablets were removed from the drum and weighed. The test was performed in triplicate for each sample.

2.7. Release Kinetics

2.7.1. Dissolution Test

The dissolution test was performed using a dissolution tester ERWEKA GmbH DT 126 light (Haan, Germany), equipped with a paddle apparatus, in purified water. The medium volume was 900 mL, the temperature was maintained at 37 ± 0.5 °C, and the paddle rotation speed was set to 50 rpm. The test was conducted on three tablets of each formulation over a period of 45 min, and it was performed in triplicate for each sample.

2.7.2. Chromatography

Quantitative analysis of the DHQ release was carried out by HPLC. Aliquots of 1 mL were withdrawn at 1, 5, 15, 30, and 45 min, followed by replacement with an equivalent volume of purified water. The peak area corresponding to a retention time of 8.4 ± 0.1 min was determined. The HPLC system used was LicArt 62 by LabConcept LLC (St. Petersburg, Russia), which included a QP-62d pump, a T-85C thermostat, a UV-62 spectrophotometric detector, a S-103dc autosampler, and an Inspire C18 column (5 µm, 150 × 4.6 mm; Dikma Technologies Inc., Foothill Ranch, CA, USA).

The mobile phase consisted of two components: component A was acetonitrile, and component B was a mixture of trifluoroacetic acid and water with pH 2.4. Elution was carried out in isocratic mode with 30% component A and 70% component B. The column

temperature was kept at 35 °C, and the flow rate was set to 0.35 mL/min. The UV detector recorded data at the maximum absorption wavelength of flavonoid, which was 288 nm. Calibration curves were constructed using three batches, each containing three concentrations of the analytes. The results are reported as mean ± standard deviation. The validation of the analytical method was performed in accordance with the recommendations of the European Pharmacopoeia.

2.7.3. Release Rate and Half-Release Period

Additionally, to describe the release kinetics of active pharmaceutical ingredient (API) from the tablets, the release rate constant ($K_{release}$) and the half-release period ($t_{50\%}$) were used. These parameters were calculated using the following equations:

$$K_{release} = \frac{C_t - C_0}{t} \quad (2)$$

$$t_{50\%} = \frac{C_0}{2 \times K_{release}} \quad (3)$$

where C_0 is the initial content of DHQ in the tablet (mg/mL), and C_t is the content of DHQ in the tablet at time t (mg/mL).

2.7.4. Difference and Similarity Factors

A comparative analysis of the drug release profiles from the tablets was performed using the difference factor (f_1, %) and the similarity factor (f_2, %), which were calculated according to the following formulas:

$$f_1 = \frac{\sum_{j=1}^{n} |R_j - T_j|}{\sum_{j=1}^{n} R_j} \times 100\% \quad (4)$$

$$f_2 = 50 \times \left\{ \left[1 + \frac{1}{n} \sum_{j=1}^{n} |R_j - T_j|^2 \right]^{-0.5} \times 100\% \right\} \quad (5)$$

where n is the number of sampling time points, and R_j and T_j are the fractions of DHQ released from the reference and test formulation at time point j.

2.8. IR-Analysis

IR-spectroscopy was performed using the attenuated total reflection (ATR) technique on an FSM 2202 Fourier transform infrared (FTIR) spectrometer (Infraspec Ltd., St. Petersburg, Russia) with an ATR crystal accessory (Infraspec Ltd., St. Petersburg, Russia), without any prior sample preparation. Data acquisition was carried out at room temperature over a wavenumber range from 4000 to 400 cm^{-1} with 2 cm^{-1} resolution. Instrument control, spectral visualization, and data processing were performed using the FSpec software (v. 4.3.1.15, Infraspec Ltd., Russia). The following samples were analyzed using the technique without adding any extra substances: initial DHQ and L-lysine, their composition (1:2, mol.), tableting masses 1 and 2, and surfaces and cross-sections of orally disintegrating tablets based on DHQ and its composition with L-lysine.

The calculation of intermolecular bond energy (ΔE, kJ/mol) was carried out according to the Badger–Bauer rule:

$$\Delta E = m \times \Delta v + c \quad (6)$$

where Δv is the difference in wavenumbers at the maxima of the absorption bands (cm^{-1}), and m and c are empirical constants (kJ·cm/mol and kJ/mol, respectively). According to

Bhatta et al. [43], these constants are equal to 0.077 kJ·cm/mol and 2.02 kJ/mol, respectively, in vacuum.

3. Results

3.1. Tablets from Formulations Based on DHQ Modifications

Tableting masses 1 and 2 (TM1 and TM2, respectively) were represented as powders. Tablets of formulations 1 and 2 (TF1 and TF2, respectively) had the same color as tableting masses and were visually distinguished by the slight yellowish hue of L-lysine.

3.2. SeDeM Expert System Analysis

The obtained results of SeDeM analysis are presented in Figure 1. Values falling below 0 were adjusted to 0, and values above 10 were capped at 10 in accordance with SeDeM charting rules.

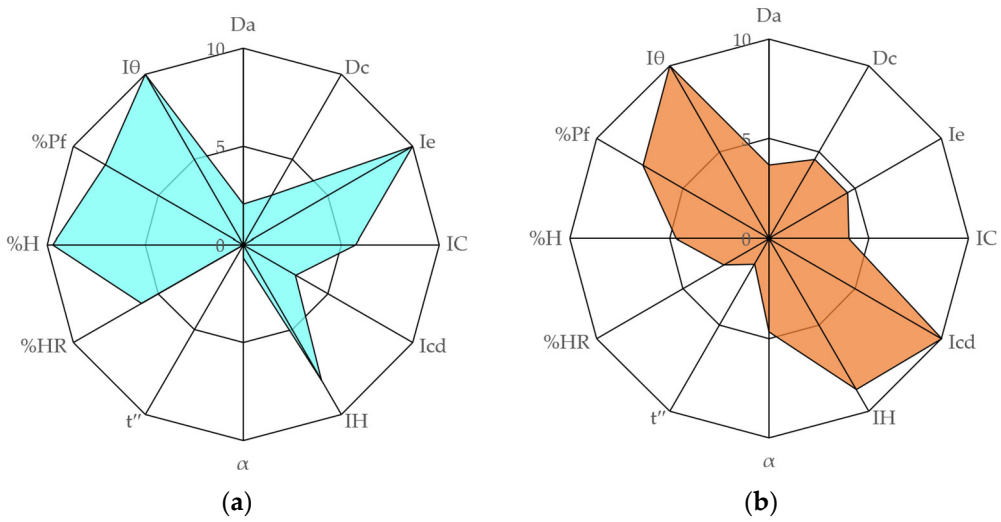

Figure 1. SeDeM graphical representation for: (**a**) DHQ; (**b**) DHQ-L-lysine composition. *Da* is bulk density, *Dc* is tapped density, *Ie* is interparticle porosity, *IC* is Carr's index, *Icd* is cohesion index, *IH* is Hausner index, *α* is angle of repose, *t''* is powder flow, %*HR* is loss of drying, %*H* is hygroscopicity, %*Pf* is particles < 50 µm, *Iθ* is homogeneity index.

The diagrams are dissimilar, being alike only on Hausner index, particles < 50 µm, and homogeneity index parameters. The most pronounced change is a maximum "spike" (10.0) in the cohesion index on the DHQ-L-lysine composition diagram, where DHQ alone is lower than five. The bottom of the DHQ diagram is almost empty: the spikes of powder flow and angle of repose barely leave the center point. In the DHQ-L-lysine composition, this area expands significantly, as these indices move closer to the acceptable threshold of five. DHQ shows excellent particle homogeneity and low hygroscopicity. On the DHQ-L-lysine composition diagram the spikes of hygroscopicity and loss on drying shrink toward the center, indicating the trade-off made for better compressibility.

Radius values and incidence of powders are presented in Table 4.

DHQ-L-lysine composition shows an improved dimensional incidence (4.12) compared to DHQ alone (2.45), due to higher bulk and tapped densities. DHQ alone exhibits extremely poor flow, with a powder flow radius of 0 and an angle of repose radius of 0.666. The DHQ-L-lysine composition significantly improves these. Although overall compressibility indices of DHQ (6.28) and DHQ-L-lysine composition (6.18) are similar, L-lysine maximizes the cohesion index to a radius of 10.0, whereas DHQ alone is deficient at 3.1. DHQ is more stable in terms of moisture, while the DHQ-L-lysine composition is significantly more hygroscopic, with its radius value dropping from 9.728 to 4.669, respectively. In

lubricity/dosage incidence, both DHQ (9.06) and DHQ-L-lysine compositions (8.65) show excellent results.

Both powders exceed the minimum IGC threshold of five, which makes them suitable for direct compression.

Table 4. SeDeM results for DHQ and DHQ-L-lysine composition.

Incidence Factor	Parameter	DHQ		DHQ-L-Lysine Composition	
		r	Incidence	*r*	Incidence
Dimensions	*Da*	2.041	2.45	3.662	4.12
	Dc	2.863		4.577	
Compressibility	*Ie*	10.000	6.28	4.549	6.18
	IC	5.742		3.998	
	Icd	3.100		10.000	
Flowability	*IH*	7.986	2.88	8.751	4.96
	α	0.666		4.666	
	t″	0		1.467	
Lubricity/Stability	*%HR*	5.979	7.85	2.622	3.65
	%H	9.728		4.669	
Lubricity/Dosage	*%Pf*	8.122	9.06	7.296	8.65
	Iθ	10.000		10.000	
IGC			5.254		5.256

3.3. Flowability Assessment

The results of flowability assessment for formulation 1 and 2 are presented in Figure 2.

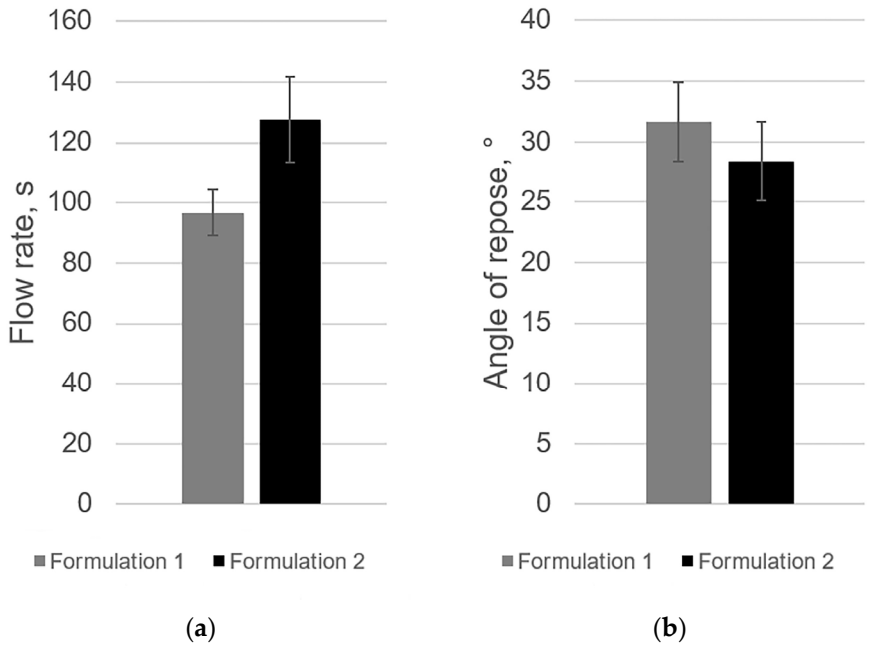

(**a**) (**b**)

Figure 2. Flowability of tableting masses: (**a**) flow rate; (**b**) angle of repose. The error bars reflect confidence interval (α 0.05) of triplicate measurement.

The mean flow rate for TM1 and TM2 was 96.67 ± 7.68 and 127.67 ± 14.02 s, respectively (Figure 2a). The flow rate of TM2 is 1.32-times higher compared to TM1, which is a significant difference. The average angle of repose rate was 31.67 ± 3.27° and 28.33 ± 3.27° (Figure 2b), so the flowability character can be determined as "good" (31–35) and "excellent" (25–30) in terms of European Pharmacopoeia for TM1 and TM2, respectively.

The difference between the formulations in these rates is 12.08% and 1.74% between TM2 and TM1 for *IC* and *IH*, respectively (Table 5).

Table 5. *IC* and *IH* of tableting masses.

	***IC*, %**	***IH***
TM1	11.72	1.13
TM2	13.33	1.15

According to the European Pharmacopoeia, the flowability of both tableting masses can be characterized as "good" (11–15% and 1.12–1.18).

3.4. Pharmaceutical–Technological Characteristics Assessment

The pharmaceutical–technological characteristics of tablets, manufactured based on the TM1 and TM2, are summarised in Table 6. TF1 disintegrated almost two times faster than TF2. For the tablets' diameter of 17.7 cm, the crushing strength of more than 50 N is decent. The friability lower than 3% is also a good result.

Table 6. Pharmaceutical–technological characteristics of tablets.

	Disintegration, min	**Crushing Strength, N**	**Friability, %**
TF1	0.90	126	1.0
TF2	1.73	119	0.2

3.5. Release Kinetics Assessment

Figure 3 represents data obtained using the validated method for DHQ in compositions containing L-lysine. The retention time of DHQ was 8.3 ± 0.1 min, while the dead time was 3.9 ± 0.1 min. During the method validation, a correlation coefficient of r 0.99997 was obtained in the analytical range from 0.0001 mg/mL to 0.1250 mg/mL, covered by the linear dependence equation $y = 155,376x - 27.632$.

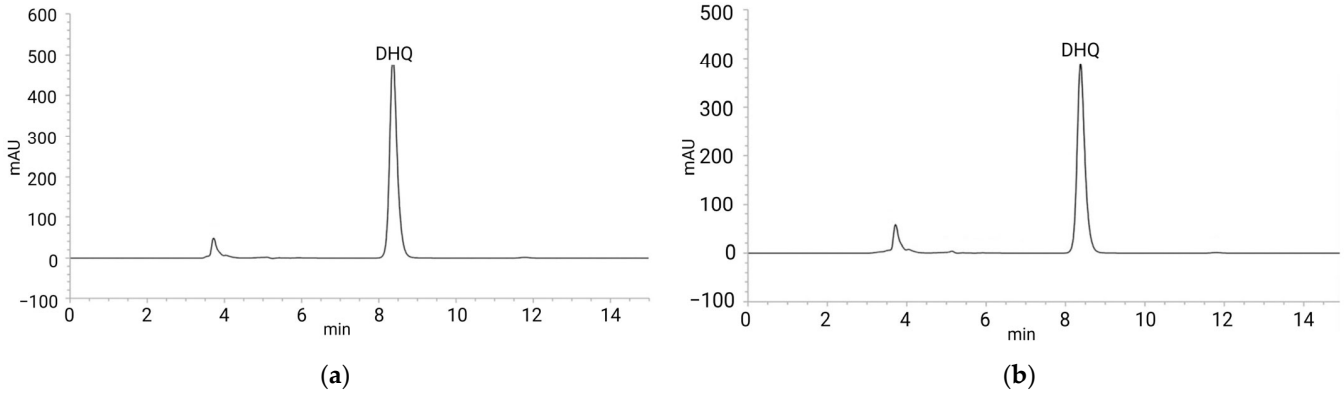

(**a**) (**b**)

Figure 3. HPLC data of dissolution test at 30 min for: (**a**) TF1; (**b**) TF2.

The repeatability, determined for each point of the calibration curve based on parallel injections of a single solution and expressed as the relative standard deviation, was less than 2% in concentrations of DHQ from 0.0001 to 0.1250 mg/mL.

For the linear dependence equation between the experimentally found and true values, the hypothesis of the slope tangent being equal to one and the intercept being equal to zero is confirmed at a confidence level of 0.05 (Table 7). That confirms the accuracy of the method.

Table 7. Confirmation of the accuracy of the quantitative analysis method for DHQ.

	Y-Intercept	Variable X1
Lower 95%	−0.00315	0.95305
Upper 95%	0.00302	1.03852

Based on HPLC data, a plot of the bioflavonoid concentration versus time was constructed (Figure 4).

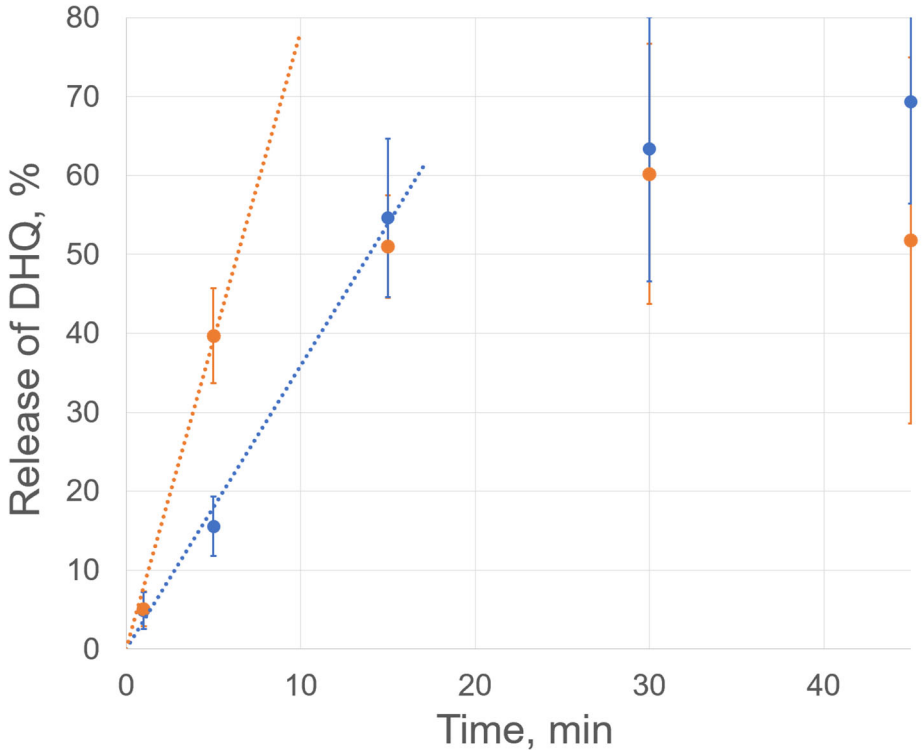

Figure 4. Release kinetics of DHQ in TF1 (orange) and TF2 (blue). The bars reflect confidence intervals (α 0.05) of triplicate measurement.

The curve reaches a plateau by 5 and 15 min for TF1 and TF2, respectively. The release rate constants ($K_{release}$) during these periods were 8.14 and 3.61 min^{-1}, respectively, while the half-release periods ($t_{50\%}$) were 6.14 and 13.85 min, respectively (Table 8). The difference factor (f_1) and the similarity factor (f_2) were calculated as 23.43% and 43.37%, respectively.

Table 8. Release kinetics characteristics.

TF	$K_{release}$, %/min	$t_{50\%}$, min	f_1, %	f_2, %
1	8.14	6.14	23.44	43.38
2	3.61	13.85		

3.6. IR-Analysis Profiles

In the IR spectra of the initial components of the tableting masses, absorption bands corresponding to their functional groups and structural elements are observed. Thus,

the spectral profile of DHQ (Figure 5a) is characterized by signals at 3394 cm^{-1} (ν_{O-H}), 1634 cm^{-1} ($\nu_{C=O}$), a series at 1614, 1587, 1516, 1448 cm^{-1} ($\nu_{Cap=Cap}$), 1479 and 1362 cm^{-1} (δ_{C-H}), 1308 cm^{-1} (δ_{O-H}), 1258 and 1163 cm^{-1} (ν_{C-O-C}).

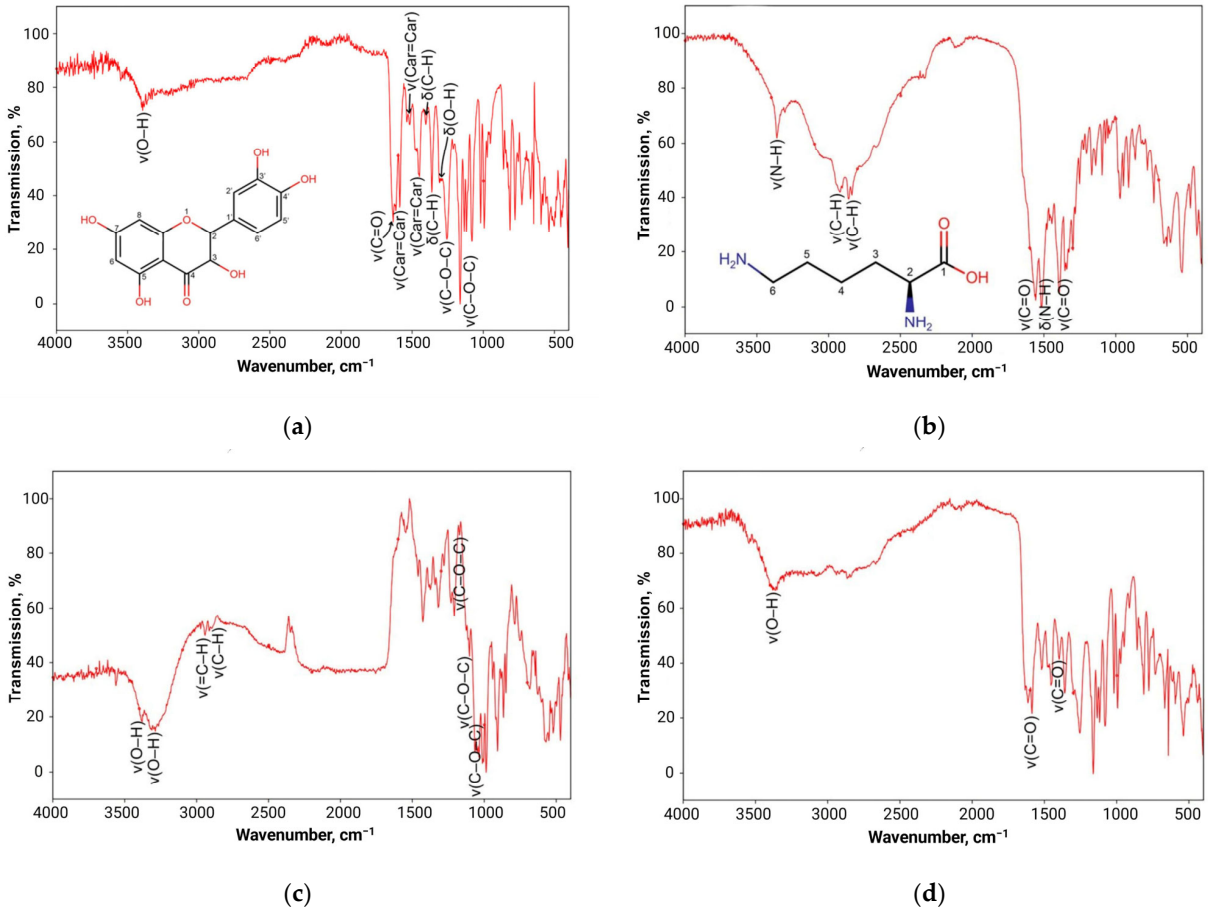

Figure 5. IR spectra of: (**a**) DHQ; (**b**) L-lysine; (**c**) excipients; (**d**) DHQ-L-lysine composition.

At the same time, the IR spectrum of L-lysine (Figure 5b) shows absorption bands at 3360 cm^{-1} (ν_{N-H}), 2920 and 2837 cm^{-1} (ν_{C-H}), 1558 and 1394 cm^{-1} ($\nu_{C=O}$), and 1520 cm^{-1} (δ_{N-H}). Sucrose is the major component in a spectrum of the excipients without API. Cellulose, mannitol, fructose, crospovidone, and ascorbic acid are also present. This explains the presence of the following signals in Figure 5c: 3379 и 3286 cm^{-1} (ν_{O-H}), 2972 cm^{-1} ($\nu_{=C-H}$), 2941 cm^{-1} (ν_{C-H}), and a series at 1173, 1126, 1113, 1103, and 1065 cm^{-1} (ν_{C-O-C}).

The IR spectrum of the DHQ-L-lysine composition (Figure 5d) is not a result of averaging the profiles of the initial compounds considering their molar ratio (*r* 0.8750). Instead, it more closely resembles the spectrum of DHQ (*r* 0.9574) than the spectrum of L-lysine (*r* 0.8267), although the amount of the amino acid is twice as high as the concentration of the flavonoid. The shift in the absorption band corresponding to ν_{O-H} to 3364 cm^{-1} is also notable, effectively merging with the ν_{N-H} signal. This, however, was accompanied by an increase in light transmittance. In the synthetic averaged spectrum, maximum intensity was observed at 3360 cm^{-1}. Additionally, the $\nu_{C=O}$ absorption bands of L-lysine shifted to a shorter-wavelength region, reaching 1562 and 1398 cm^{-1}.

Blending of the excipients and API did not cause significant changes in the spectral profiles (Figure 6), given that the proportion of excipients in the mixture was 96.8% and 93.4% by mass for TF1 and TF2, respectively. The correlation coefficient between the spectral profiles of the formulations was 0.9639.

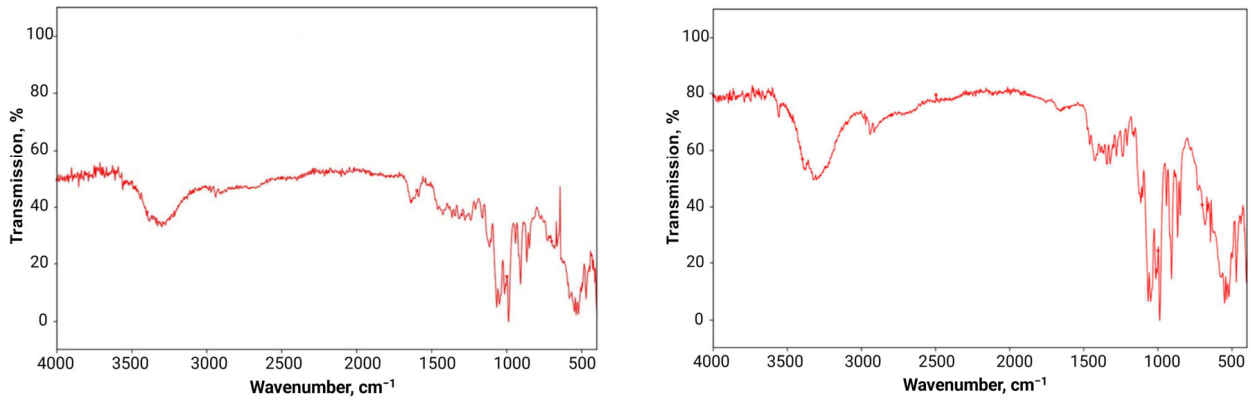

Figure 6. IR spectra of tableting masses: (**a**) TM1; (**b**) TM2.

The tablet manufacture had a more critical impact on the characteristics of the IR spectra (Figure 7). Compared to the initial tablet masses, the r values were −0.8785 and 0.5474 for TF1 and TF2, respectively. A common feature of the IR spectra of the tablets in the cross-section was the shift in the broad absorption band in the hydrogen-bonding region by an average of 295 cm^{-1}, compared to the spectra of the initial tablet masses.

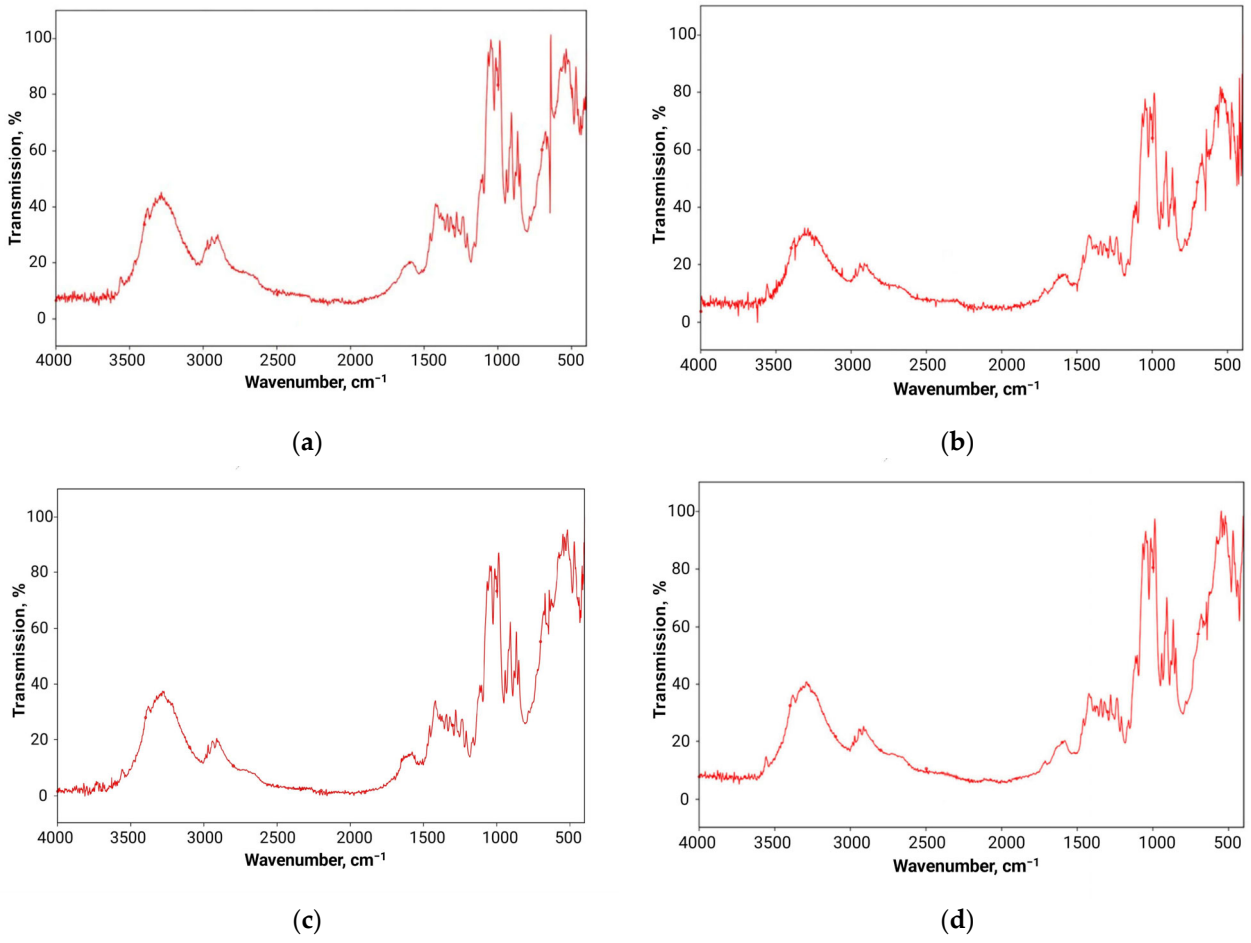

Figure 7. IR spectra of tablet surfaces and cross-sections: (**a**) TF1 surface; (**b**) TF2 surface; (**c**) TF1 cross-section; (**d**) TF2 cross-section.

At the same time, the spectra recorded from the tablet surface and cross-section were more consistent with each other: for TF1 and TF2, the correlation coefficient was 0.9766 and 0.9899, respectively. Moreover, the spectral profiles of TF1 were closer to those of tablets without API than those in TF2.

In addition, the IR spectrum of TF1 was characterized by a shift in the absorption band corresponding to ν_{O-H} toward a shorter wavelength, relative to the TF2. The wavenumber shift (Δv) was 21 cm^{-1} on the surface and 4 cm^{-1} in the cross-section.

4. Discussion

This research was performed to design orally disintegrating tablets based on the DHQ composition with L-lysine and assess the impact of amino acids on the characteristics of the final dosage form.

Previously, two pharmaceuticals based on DHQ were registered in Russia: Diquertin [44] and Ascovertin [45]. Both were in the form of tablets where potato starch and powdered sugar were used as excipients. Stearic acid was employed as an anti-friction component. Later, orally disintegrating tablets based on amorphous DHQ were developed [46]. In addition to sucrose, menthol was added to mask the bitter taste of the flavonoid. Also, crospovidon was added to optimize the disintegration time. In contrast, one article reports on tablets with DHQ which contained siliconized MCC used as an excipient, and sodium starch glycolate and Aerosil 200 as disintegrants [47].

Based on a summary of data on the excipients of orally disintegrating tablets [48], it was suggested to return to the initial formulation: sucrose makes up more than two-thirds of the tablet mass, additionally masking the bitter taste of DHQ and L-lysine. PROSOLV® ODT G2 was employed as a disintegrant. Ascorbic acid was added to protect the flavonoid from oxidation, as the latter is characterized by a higher redox potential: for ascorbic acid and DHQ this parameter is −0.17 V and 0.50 V, respectively [49].

As for the SeDeM analysis, addition of L-lysine to DHQ significantly improved the dimensional and flowability profiles. It maximized the cohesion index, which can be connected with the formation of stronger intermolecular bonds. Both powders show excellent results in the lubricity/dosage incidence. The lubricity/stability incidence is the only factor where the DHQ-L-lysine composition performs worse than DHQ. The lower value (3.65) for the composition is primarily due to its increased hygroscopicity, as L-lysine tends to attract moisture. This indicates that while the composition is superior for manufacturing, the final product may require moisture-protective packaging to maintain long-term stability.

The optimization of formulations was performed based on the properties of the resulting tablets, particularly compressibility [50,51]. Flowability of tableting masses is a key parameter in tablet manufacture [51,52]. The obtained results demonstrate that the DHQ modification with L-lysine significantly improves this parameter. A 32% increase in flow rate and a reduction in the angle of repose to the "excellent" flow category confirm the advantages of TF2. Compared to previous orally disintegrating tablets, the new formulations are characterized by higher strengths and friability [46]. Pharmaco-technological parameters of the finished tablets showed that TF2 exhibits more stable characteristics. Despite the longer disintegration time of TF2 (almost twice as long as TF1), the tablet strength remains within the normal range (119 N), and friability is at a low level (0.2%, five times lower than in TF1). These observations may be explained by a crystalline nature of amino acid particles [53], that are quite flexible and act as a mold. However, the impact of compression force was outside the scope of the current study, so it should be investigated in future work, as the tableting parameters may have a significant impact on characteristics of

the finished dosage form (including tablet strength), as is it was shown by Casian et al. [54], Donea et al. [55], Tishkov et al. [56], etc.

To assess the release profile of DHQ, a quantitative analytical method was developed using HPLC-UV and validated in accordance with the European Pharmacopoeia by the following parameters: "Specificity", "Accuracy", "Repeatability", "Analytical range", and "Linearity". A mixture of acetonitrile and water is widely used in chromatography of flavonoids, with acids as phase modifiers to reduce the ionization of phenolic groups [57–59]. The isocratic mode was explored to increase the sensitivity and accuracy of the measurement [60] that may be critical in case of a release profile assessment. In this research, no effect of amino acid on flavonoid quantitative analysis was detected.

Both release profiles are described by the zero-order kinetic curve, which is common for tablets [61–63]. The release profile of DHQ shows significant differences between the tablets. A slower but more gradual release of DHQ from TF2 (half-release period of 13.85 min, nearly twice as long as in TF1), which correlates with disintegration time, may provide a prolonged drug action. The difference factor value (23.43%) and similarity factor value (43.37%) indicate substantial differences in release kinetics, being higher than 15% and lower than 50%, respectively. The prolonged release profile of TF2 can be explained by a higher strength of the tablets, explained by the presence of L-lysine. A longer half-release period may be more appropriate for topical pharmaceuticals applied in the oral cavity [64,65]. It is important to note that the values of stability and bioavailability are more essential for the design of orally disintegrating tablets [66–68], so TF2 seems to be more promising for the further translation in the industry.

The obtained IR spectra of the initial compounds are well explained by the structure of DHQ and L-lysine, and are consistent with literature data [24] (DHQ, Figure 5), [69] (Lys, Figure 3).

Based on the shift in absorption bands corresponding to ν_{O-H} in DHQ and $\nu_{C=O}$ in L-lysine observed in the IR spectrum of the composition, it can be assumed that during the composition's preparation, a mechanochemical activation process occurs, leading to the formation of weak intermolecular hydrogen bonds (4.3 kJ/mol) between the phenolic hydroxyl groups of the flavonoid and the ionized carboxyl group of the amino acid. Previously, Skakunova and Rychkov reported on the change in absorption bands in Raman spectra of L-leucine hydrogen maleate after treatment of the crystals by different pressures. It was explained by changes in the intermolecular interactions, which correlates with the amorphization of crystal material [70]. However, shifts in spectral signals were also observed without a change in the phase state, which was explained by the impact of the phase on the bond vibrations.

Based on the Badger–Bauer rule, it was suggested that in the current research the tablet compression led to the formation of stronger intermolecular bonds—24.7 kJ/mol. The bonds in tablets with the composition were up to 3.6 kJ/mol stronger than those in TF1. The observed spectral changes may also be explained by the influence of L-lysine on the properties of the solid phase. Notably, the spectral analysis results correlate with the pharmaceutical–technological characteristics of the tablets: TF1 disintegrated faster, whereas TF2 exhibited greater mechanical strength. Nevertheless, this phenomenon requires further investigation under different tableting conditions. Probably, IR and Raman spectroscopy may be valuable analytical techniques in the early stages of pharmaceutical development.

5. Conclusions

The obtained results have important practical implications for the development of new dosage forms with DHQ. SeDeM expert system results showed that from a manufacturing

perspective, the DHQ-L-lysine composition is more advanced. The modification with L-lysine not only improves technological characteristics but also has the potential to provide a more stable therapeutic local concentration of the active substance. Thus, the conducted study demonstrates the promise of using the DHQ-L-lysine composition for developing effective dosage forms with improved technological characteristics and controlled release of the active substance for local application.

Author Contributions: Conceptualization, R.P.T., M.N.A. and I.A.S.; methodology, R.P.T., A.A.S. and M.N.A.; software, M.N.A.; validation, R.P.T., A.A.S., M.N.A. and I.A.S.; formal analysis, R.P.T., M.D.K. and A.A.S.; investigation, M.D.K. and E.V.K.; resources, G.Y.E.; data curation, M.D.K.; writing—original draft preparation, R.P.T., M.D.K. and E.V.K.; writing—review and editing, A.A.S., G.Y.E., M.N.A. and I.A.S.; visualization, R.P.T. and M.D.K.; supervision, M.N.A. and I.A.S.; project administration, R.P.T. and M.D.K.; funding acquisition, R.P.T. All authors have read and agreed to the published version of the manuscript.

Funding: This research was funded by the Russian Science Foundation, grant number 25-75-00071, https://rscf.ru/en/project/25-75-00071/ (accessed on 12 April 2026).

Institutional Review Board Statement: Not applicable.

Informed Consent Statement: Not applicable.

Data Availability Statement: The original contributions presented in this study are included in the article. Further inquiries can be directed to the corresponding author.

Conflicts of Interest: The authors declare no conflicts of interest.

Abbreviations

The following abbreviations are used in this manuscript:

API	Active pharmaceutical ingredient
DHQ	Dihydroquercetin
CQAs	Critical quality attributes
IGC	Good compression index
IPP	Parametric profile index
SeDeM	Sediment Delivery Model
TF1 and TF2	Tablets of formulation 1 and 2
TM1 and TM2	Tableting masses 1 and 2
QTPP	Quality Target Product Profile

References

1. Dye, B.A. The Global Burden of Oral Disease: Research and Public Health Significance. *J. Dent. Res.* **2017**, *96*, 361–363. [CrossRef] [PubMed]
2. Onerova, A.; Yeslyamgaliyeva, A. Prevalence of Inflammatory Periodontal Diseases. *Przegl Epidemiol.* **2024**, *78*, 182–192. [CrossRef] [PubMed]
3. Jin, L.; Lamster, I.; Greenspan, J.; Pitts, N.; Scully, C.; Warnakulasuriya, S. Global Burden of Oral Diseases: Emerging Concepts, Management and Interplay with Systemic Health. *Oral Dis.* **2016**, *22*, 609–619. [CrossRef] [PubMed]
4. Salminen, A.; Maatta, A.M.; Mantyla, P.; Leskela, J.; Pietiainen, M.; Buhlin, K.; Suominen, A.L.; Paju, S.; Sattler, W.; Sinisalo, J.; et al. Systemic Metabolic Signatures of Oral Diseases. *J. Dent. Res.* **2024**, *103*, 13–21. [CrossRef] [PubMed]
5. Bitencourt, F.V.; Nascimento, G.G.; Costa, S.A.; Andersen, A.; Sandbæk, A.; Leite, F.R.M. Co-Occurrence of Periodontitis and Diabetes-Related Complications. *J. Dent. Res.* **2023**, *102*, 1088–1097. [CrossRef] [PubMed]
6. Cekici, A.; Kantarci, A.; Hasturk, H.; Van Dyke, T.E. Inflammatory and Immune Pathways in the Pathogenesis of Periodontal Disease. *Periodontol. 2000* **2014**, *64*, 57–80. [CrossRef] [PubMed]
7. Mo, J.-J.; Lai, Y.-R.; Huang, Q.-R.; Li, Y.-R.; Zhang, Y.-J.; Chen, R.-Y.; Qian, S.-J. Single-Cell Sequencing Identifies Inflammation-Promoting Fibroblast-Neutrophil Interaction in Peri-Implantitis. *J. Clin. Periodontol.* **2024**, *51*, 196–208. [CrossRef] [PubMed]
8. Hasturk, H.; Kantarci, A.; Van Dyke, T.E. Oral Inflammatory Diseases and Systemic Inflammation: Role of the Macrophage. *Front. Immunol.* **2012**, *3*, 118. [CrossRef] [PubMed]

9. Sanz, I.; Alonso, B.; Carasol, M.; Herrera, D.; Sanz, M. Nonsurgical Treatment of Periodontitis. *J. Evid. Based Dent. Pract.* **2012**, *12*, 76–86. [CrossRef] [PubMed]
10. Teughels, W.; Dhondt, R.; Dekeyser, C.; Quirynen, M. Treatment of Aggressive Periodontitis. *Periodontol. 2000* **2014**, *65*, 107–133. [CrossRef] [PubMed]
11. Marsh, P.D. Role of the Oral Microflora in Health. *Microb. Ecol. Health Dis.* **2000**, *12*, 130–137. [CrossRef]
12. Sullivan, Å.; Edlund, C.; Nord, C.E. Effect of Antimicrobial Agents on the Ecological Balance of Human Microflora. *Lancet Infect. Dis.* **2001**, *1*, 101–114. [CrossRef] [PubMed]
13. Ayinde, O.; Ross, J.D. The Frequency and Duration of Side-Effects Associated with the Use of Oral Metronidazole; A Prospective Study of VITA Trial Participants. *Int. J. STD AIDS* **2023**, *34*, 897–902. [CrossRef] [PubMed]
14. Clarkson, J.E.; Young, L.; Ramsay, C.R.; Bonner, B.C.; Bonetti, D. How to Influence Patient Oral Hygiene Behavior Effectively. *J. Dent. Res.* **2009**, *88*, 933–937. [CrossRef] [PubMed]
15. Graziani, F.; Karapetsa, D.; Alonso, B.; Herrera, D. Nonsurgical and Surgical Treatment of Periodontitis: How Many Options for One Disease? *Periodontol. 2000* **2017**, *75*, 152–188. [CrossRef] [PubMed]
16. Fang, Y.; Cao, W.; Xia, M.; Pan, S.; Xu, X. Study of Structure and Permeability Relationship of Flavonoids in Caco-2 Cells. *Nutrients* **2017**, *9*, 1301. [CrossRef] [PubMed]
17. Schauss, A.G.; Tselyico, S.S.; Kuznetsova, V.A.; Yegorova, I. Toxicological and Genotoxicity Assessment of a Dihydroquercetin-Rich Dahurian Larch Tree (Larix Gmelinii Rupr) Extract (Lavitol). *Int. J. Toxicol.* **2015**, *34*, 162–181. [CrossRef] [PubMed]
18. Liu, Z.; Qiu, D.; Yang, T.; Su, J.; Liu, C.; Su, X.; Li, A.; Sun, P.; Li, J.; Yan, L.; et al. Research Progress of Dihydroquercetin in the Treatment of Skin Diseases. *Molecules* **2023**, *28*, 6989. [CrossRef] [PubMed]
19. Terekhov, R.P.; Selivanova, I.A.; Anurova, M.N.; Zhevlakova, A.K.; Nikitin, I.D.; Cong, Z.; Ma, S.; Yang, F.; Dong, Z.; Liao, Y. Comparative Study of Wound-Healing Activity of Dihydroquercetin Pseudopolymorphic Modifications. *Bull. Exp. Biol. Med.* **2021**, *170*, 444–447. [CrossRef] [PubMed]
20. Alam, Q.; Krishnamurthy, S. Dihydroquercetin Ameliorates LPS-Induced Neuroinflammation and Memory Deficit. *Curr. Res. Pharmacol. Drug Discov.* **2022**, *3*, 100091. [CrossRef] [PubMed]
21. Lei, L.; Chai, Y.; Lin, H.; Chen, C.; Zhao, M.; Xiong, W.; Zhuang, J.; Fan, X. Dihydroquercetin Activates AMPK/Nrf2/HO-1 Signaling in Macrophages and Attenuates Inflammation in LPS-Induced Endotoxemic Mice. *Front. Pharmacol.* **2020**, *11*, 662. [CrossRef] [PubMed]
22. Wang, Y.-H.; Wang, W.-Y.; Chang, C.-C.; Liou, K.-T.; Sung, Y.-J.; Liao, J.-F.; Chen, C.-F.; Chang, S.; Hou, Y.-C.; Chou, Y.-C.; et al. Taxifolin Ameliorates Cerebral Ischemia-Reperfusion Injury in Rats Throughits Anti-Oxidative Effect and Modulation of NF-Kappa B Activation. *J. Biomed. Sci.* **2006**, *13*, 127–141. [CrossRef] [PubMed]
23. Liu, Y.; Shi, X.; Tian, Y.; Zhai, S.; Liu, Y.; Xiong, Z.; Chu, S. An Insight into Novel Therapeutic Potentials of Taxifolin. *Front. Pharmacol.* **2023**, *14*, 1173855. [CrossRef] [PubMed]
24. Zu, Y.; Wu, W.; Zhao, X.; Li, Y.; Wang, W.; Zhong, C.; Zhang, Y.; Zhao, X. Enhancement of Solubility, Antioxidant Ability and Bioavailability of Taxifolin Nanoparticles by Liquid Antisolvent Precipitation Technique. *Int. J. Pharm.* **2014**, *471*, 366–376. [CrossRef] [PubMed]
25. Yang, D.; Zhu, R.; Xu, H.-X.; Zhang, Q.-F. Antibacterial Mechanism of Taxifolin and Its Application in Milk Preservation. *Food Biosci.* **2023**, *53*, 102811. [CrossRef]
26. Unver, T. The Inhibitory Effects of Taxifolin, Namely Dihydroquercetin as a Pharmaceutical Agent on the Growth of Bacterial and Fungal Species. *Ann. Med. Res.* **2024**, *31*, 222. [CrossRef]
27. Orlova, S.V.; Tatarinov, V.V.; Nikitina, E.A.; Sheremeta, A.V.; Ivlev, V.A.; Vasil'ev, V.G.; Paliy, K.V.; Goryainov, S.V. Bioavailability and Safety of Dihydroquercetin (Review). *Pharm. Chem. J.* **2022**, *55*, 1133–1137. [CrossRef] [PubMed]
28. Zhang, Y.; Yu, J.; Dong, X.-D.; Ji, H.-Y. Research on Characteristics, Antioxidant and Antitumor Activities of Dihydroquercetin and Its Complexes. *Molecules* **2018**, *23*, 20. [CrossRef] [PubMed]
29. Colombo, M.; Michels, L.R.; Teixeira, H.F.; Koester, L.S. Flavonoid Delivery by Solid Dispersion: A Systematic Review. *Phytochem. Rev.* **2022**, *21*, 783–808. [CrossRef]
30. Krasnyuk, I.; Koval'skii, I.; Nikulina, O.; Belyatskaya, A.; Kharitonov, Y.; Grikh, V.; Korol, L.; Obidchenko, Y.; Vorob'ev, A. Preparation and Investigation of Tabletted Medicinal Formulations of a Solid Dispersion of Rutin. *Pharm. Chem. J.* **2015**, *49*, 481–485. [CrossRef]
31. Terekhov, R.P.; Ilyasov, I.R.; Beloborodov, V.L.; Zhevlakova, A.K.; Pankov, D.I.; Dzuban, A.V.; Bogdanov, A.G.; Davidovich, G.N.; Shilov, G.V.; Utenyshev, A.N.; et al. Solubility Enhancement of Dihydroquercetin via "Green" Phase Modification. *Int. J. Mol. Sci.* **2022**, *23*, 15965. [CrossRef] [PubMed]
32. Lin, S.; Wang, Y.; Huang, C.; Niu, Y.; Liu, Y.; Xiao, W.; Chen, F.; Xue, R. Co-Amorphous Salts of Luteolin-Arginine/Lysine with Enhanced Solubility. *Mater. Chem. Phys.* **2026**, *352*, 132014. [CrossRef]

33. Tretyakova, I.S.; Rychkov, D.A.; Kil'met'ev, A.S.; Lomovskiy, I.O. Computational Study of Chemical Phenol Glycosylation Mechanism in the Gas Phase for Modeling Direct Glycoconjugate Formation in Raw Plant Material. *Comput. Theor. Chem.* **2023**, *1225*, 114182. [CrossRef]
34. Li, H.; Ma, W.; Lyv, Y.; Gao, S.; Zhou, J. Glycosylation Modification Enhances (2S)-Naringenin Production in Saccharomyces Cerevisiae. *ACS Synth. Biol.* **2022**, *11*, 2339–2347. [CrossRef] [PubMed]
35. Smith, A.J.; Kavuru, P.; Wojtas, L.; Zaworotko, M.J.; Douglas Shytle, R. Cocrystals of Quercetin with Improved Solubility and Oral Bioavailability. *Mol. Pharm.* **2011**, *8*, 1867–1876. [CrossRef] [PubMed]
36. Puspita, O.; Salam, R.; Sulistyowaty, M.; Setyawan, D. Rational Cocrystal Design of Hesperetin Using Integrated Molecular Docking, SAPT, and DFT Approach. *Trop. J. Nat. Product. Res.* **2026**, *10*, 7772. [CrossRef]
37. Zhang, C.; He, Y.; Shen, Y. L-Lysine Protects against Sepsis-Induced Chronic Lung Injury in Male Albino Rats. *Biomed. Pharmacother.* **2019**, *117*, 109043. [CrossRef] [PubMed]
38. Svotin, A.A.; Korochkina, M.D.; Kolesnikova, D.R.; Krivosheeva, E.A.; Terekhov, R.P.; Selivanova, I.A. Bioavailability and Cytotoxicity of Dihydroquercetin—L-Lysine Compositions. *Pharmacy* **2025**, *8*, 31–39. [CrossRef]
39. Svotin, A.A.; Taldaev, A.; Nikitin, I.D.; Korochkina, M.D.; Terekhov, R.P.; Selivanova, I.A. Insights in Wound Healing Properties of Water-Soluble Composition of Dihydroquercetin and L-Lysine. *J. Pharm. Pharm. Sci.* **2025**, *28*, 13831. [CrossRef] [PubMed]
40. ICH Q8 (R2) Pharmaceutical Development—Scientific Guideline | European Medicines Agency (EMA). Available online: https://www.ema.europa.eu/en/ich-q8-r2-pharmaceutical-development-scientific-guideline (accessed on 14 May 2026).
41. Canadell-Heredia, R.; Rouaz-El-Hajoui, K.; Franco-Piedrahita, N.; Pérez-Lozano, P.; Suñé-Pou, M.; Suñé-Negre, J.M.; García-Montoya, E. Preformulation Study of Carbamazepine Orally Disintegrating Tablets for Pediatric Patients Using Direct Compression and the SeDeM Diagram Tool: A Quality by Design Approach. *Pharmaceutics* **2025**, *17*, 624. [CrossRef] [PubMed]
42. European Pharmacopoeia Online. Available online: https://pheur-online.edqm.eu/home/ (accessed on 14 May 2026).
43. Bhatta, R.S.; Iyer, P.P.; Dhinojwala, A.; Tsige, M. A Brief Review of Badger–Bauer Rule and Its Validation from a First-Principles Approach. *Mod. Phys. Lett. B* **2014**, *28*, 1430014. [CrossRef]
44. Kolhir, V.K.; Bykov, V.A.; Teselkin, Y.O.; Babenkova, I.V.; Tjukavkina, N.A.; Rulenko, I.A.; Kolesnik, Y.A.; Eichholz, A.A. Use of a New Antioxidant Diquertin as an Adjuvant in the Therapy of Patients with Acute Pneumonia. *Phytother. Res.* **1998**, *12*, 606–608. [CrossRef]
45. Plotnikov, M.B.; Plotnikov, D.M.; Aliev, O.I.; Maslov, M.Y.; Vasiliev, A.S.; Alifirova, V.M.; Tyukavkina, N.A. Hemorheological and Antioxidant Effects of Ascovertin in Patients with Sclerosis of Cerebral Arteries. *Clin. Hemorheol. Microcirc.* **2004**, *30*, 449–452. [PubMed]
46. Terekhov, R.P.; Anurova, M.N.; Selivanova, I.A. The Impact of the Phase State of Dihydroquercetin on the Pharmacological and Technological Properties of Lozenges. *Pharmacy* **2020**, *69*, 44–49. [CrossRef]
47. Abdulrazzak, S.A.; Vorobyev, A.N.; Sinitsyna, N.I.; Sharutin, I.V.; Menshova, O.V.; Elizarova, E.V.; Ivanov, Y.V.; Karamyan, A.S.; Abramovich, R.A.; Potanina, O.G.; et al. Development of dihydroquercetin-based oral tablets and evalution of the general toxic effect. *Drug Dev. Regist.* **2022**, *11*, 126–138. [CrossRef]
48. Mizina, P.G.; Gulenkov, A.S. The Orally Disintegrating Tablets: The Achievements and Prospects (Review). *Probl. Bio Med. Pharm. Chem.* **2018**, *21*, 3–11. [CrossRef]
49. Plotnikov, M.B.; Tyukavkina, N.A.; Plotnikova, T.M. *Diquertin-Based Drugs*; National Research Tomsk State University: Tomsk, Russia, 2005.
50. Yu, Y.; Zhao, L.; Lin, X.; Wang, Y.; Feng, Y. A Model to Simultaneously Evaluate the Compressibility and Compactibility of a Powder Based on the Compression Ratio. *Int. J. Pharm.* **2020**, *577*, 119023. [CrossRef] [PubMed]
51. Fassihi, A.R.; Kanfer, I. Effect of Compressibility and Powder Flow Properties on Tablet Weight Variation. *Drug Dev. Ind. Pharm.* **1986**, *12*, 1947–1966. [CrossRef]
52. Mehrotra, A.; Chaudhuri, B.; Faqih, A.; Tomassone, M.S.; Muzzio, F.J. A Modeling Approach for Understanding Effects of Powder Flow Properties on Tablet Weight Variability. *Powder Technol.* **2009**, *188*, 295–300. [CrossRef]
53. Boldyreva, E. Crystalline Amino Acids. In *Proceedings of the Models, Mysteries and Magic of Molecules*; Boeyens, J.C.A., Ogilvie, J.F., Eds.; Springer Netherlands: Dordrecht, The Netherlands, 2008; pp. 167–192.
54. Casian, T.; Iurian, S.; Gavan, A.; Negoi, O.; Marusca, D.; Marina, A.; Suciu, M.; Muntean, D.; Porfire, A.; Pop, A.L.; et al. Bridging Material Variability and Tablet Performance: Optimization of Direct Compression Using Tensile Strength–Ejection Stress Mapping. *Pharmaceutics* **2026**, *18*, 357. [CrossRef] [PubMed]
55. Donea, C.; Ciobanu, A.-M.; Cristian, D.A.; Popa, D.E.; Burcea-Dragomiroiu, G.T.A.; Hirju, M.; Draganescu, D.; Craciun, P.; Lupuliasa, D. Determination of the Impact of the Compression Force by Evaluating the Mechanical and Release Properties of Mesalazine Tablets. *Farmacia* **2022**, *70*, 964. [CrossRef]
56. Tishkov, S.; Blynskaya, E.; Alekseev, K.; Dorofeev, V. Optimization Using Regression Analysis of the Wet Granulation Process for Production of GSB-106 Tablets. *Pharm. Chem. J.* **2024**, *58*, 1315–1320. [CrossRef]

57. Poluyanov, A.M.; Sokolova, A.Y.; Koynova, A.-D.; Kulikova, S.D.; Malashenko, E.A.; Bobkova, N.V. Identification and Quantitative Determination of Flavonoids by HPLC-UV Method in the Raw Materials of Some Representatives of the Genus Rumex of Three Vegetation Time. *Drug Dev. Regist.* **2023**, *12*, 134–142. [CrossRef]
58. Gerasimov, M.A.; Perova, I.B.; Eller, K.I.; Akimov, M.Y.; Sukhanova, A.M.; Rodionova, G.M.; Ramenskaya, G.V. Investigation of Polyphenolic Compounds in Different Varieties of Black Chokeberry Aronia Melanocarpa. *Molecules* **2023**, *28*, 4101. [CrossRef] [PubMed]
59. Kurkin, V.A.; Zimenkina, N.I. HPLC Determination of Myricitrin in *Juglans nigra* L. Bark. *Pharm. Chem. J.* **2021**, *55*, 881–885. [CrossRef]
60. Gritti, F.; Guiochon, G. Accuracy and Precision of Adsorption Isotherm Parameters Measured by Dynamic HPLC Methods. *J. Chromatogr. A* **2004**, *1043*, 159–170. [CrossRef] [PubMed]
61. Wray, P.; Li, J.; Li, L.Q.; Kazarian, S.G. Combined Study of Biphasic and Zero-Order Release Formulations with Dissolution Tests and ATR–FTIR Spectroscopic Imaging. *J. Pharm. Sci.* **2014**, *103*, 1995–2004. [CrossRef] [PubMed]
62. Abdelbary, A.; El-Gazayerly, O.N.; El-Gendy, N.A.; Ali, A.A. Floating Tablet of Trimetazidine Dihydrochloride: An Approach for Extended Release with Zero-Order Kinetics. *AAPS PharmSciTech* **2010**, *11*, 1058–1067. [CrossRef] [PubMed]
63. Huang, H.; Wu, Z.; Qi, X.; Zhang, H.; Chen, Q.; Xing, J.; Chen, H.; Rui, Y. Compression-Coated Tablets of Glipizide Using Hydroxypropylcellulose for Zero-Order Release: In Vitro and in Vivo Evaluation. *Int. J. Pharm.* **2013**, *446*, 211–218. [CrossRef] [PubMed]
64. Paderni, C.; Compilato, D.; Giannola, L.I.; Campisi, G. Oral Local Drug Delivery and New Perspectives in Oral Drug Formulation. *Oral Surg. Oral Med. Oral Pathol. Oral Radiol.* **2012**, *114*, e25–e34. [CrossRef] [PubMed]
65. Ratnaparkhi, M.P.; Gupta Jyoti, P. Sustained Release Oral Drug Delivery System—An Overview. *Int. J. Pharma Res. Rev.* **2013**, *2*, 11–21.
66. Kushnazarova, R.; Mirgorodskaya, A.; Bushmeleva, K.; Vyshtakalyuk, A.; Lenina, O.; Petrov, K.; Zakharova, L. Improving the Stability, Water Solubility, and Antioxidant Activity of α-Tocopherol by Encapsulating It into Niosomes Modified with Cationic Carbamate-Containing Surfactants. *Langmuir* **2024**, *40*, 22684–22692. [CrossRef] [PubMed]
67. Noskov, S.; Parulya, O.; Lutskova, L.; Arefeva, A.; Protsenko, E.; Banko, V.; Radaeva, K.; Matvienko, I.; Gefen, M.; Karnakova, P.; et al. Bioequivalence and Safety of Generic Glecaprevir/Pibrentasvir Compared to a Branded Product: A Randomized, Crossover Study in Healthy Volunteers. *Clin. Pharmacol. Drug Dev.* **2024**, *13*, 1331–1338. [CrossRef] [PubMed]
68. Ghoshal, G. Nutraceutical Delivery Vehicles: Enhanced Stability, Bioavailability. *Food Sci. Biotechnol.* **2025**, *34*, 31–48. [CrossRef] [PubMed]
69. Kitadai, N.; Yokoyama, T.; Nakashima, S. In Situ ATR-IR Investigation of L-Lysine Adsorption on Montmorillonite. *J. Colloid Interface Sci.* **2009**, *338*, 395–401. [CrossRef] [PubMed]
70. Skakunova, K.; Rychkov, D. Low Temperature and High-Pressure Study of Bending L-Leucinium Hydrogen Maleate Crystals. *Crystals* **2021**, *11*, 1575, Correction in *Crystals* **2022**, *12*, 580. https://doi.org/10.3390/cryst12050580.. [CrossRef]